ANNUAL REVIEWS

Annual Review of Earth and Planetary Sciences

Induced Seismicity

Katie M. Keranen[1] and Matthew Weingarten[2,3]

[1]Department of Earth and Atmospheric Sciences, Cornell University, Ithaca, New York 14853, USA; email: keranen@cornell.edu

[2]Department of Geophysics, Stanford University, Stanford, California 94305, USA

[3]Department of Geological Sciences, San Diego State University, San Diego, California 92182, USA

ANNUAL REVIEWS Further

Click here to view this article's online features:
• Download figures as PPT slides
• Navigate linked references
• Download citations
• Explore related articles
• Search keywords

Keywords

induced seismicity, earthquakes, triggering

Abstract

The ability of fluid-generated subsurface stress changes to trigger earthquakes has long been recognized. However, the dramatic rise in the rate of human-induced earthquakes in the past decade has created abundant opportunities to study induced earthquakes and triggering processes. This review briefly summarizes early studies but focuses on results from induced earthquakes during the past 10 years related to fluid injection in petroleum fields. Study of these earthquakes has resulted in insights into physical processes and has identified knowledge gaps and future research directions. Induced earthquakes are challenging to identify using seismological methods, and faults and reefs strongly modulate spatial and temporal patterns of induced seismicity. However, the similarity of induced and natural seismicity provides an effective tool for studying earthquake processes. With continuing development of energy resources, increased interest in carbon sequestration, and construction of large dams, induced seismicity will continue to pose a hazard in coming years.

INTRODUCTION

Induced seismicity, also known as anthropogenic seismicity, is triggered by subsurface stress changes resulting from processes including fluid injection, fluid withdrawal, mining, and reservoir impoundment. It is likely to continue in upcoming decades as development continues in the fields of conventional and nonconventional petroleum, coalbed methane extraction, geothermal energy in igneous (e.g., Majer et al. 2007) and sedimentary (e.g., Tester et al. 2006) rocks, and geological carbon sequestration (e.g., Bachu 2008, Benson & Cole 2008, Bickle 2009).

A number of prior review articles and reports have addressed induced seismicity (e.g., Nicholson & Wesson 1992; Majer et al. 2007; Suckale 2009, 2010; Ellsworth 2013; Natl. Res. Counc. 2013; Grigoli et al. 2017). Others have addressed hydraulic fracturing (e.g., Jackson et al. 2014, Norris et al. 2016). Many of the earlier reviews were published prior to the recent dramatic increase in induced seismicity and provide thorough summaries of the state of induced seismicity prior to or at the beginning of the recent, rapid surge. Foulger et al. (2017) presented a database of all induced or potentially induced seismicity caused by anthropogenic sources to the present day. The present review therefore avoids providing an exhaustive listing of all recent or possible cases of induced seismicity, instead referring readers to these existing compilations, and focuses on (*a*) the region of impact of pore pressure from high-volume wells laterally and vertically; (*b*) the importance of local geology in modulating induced seismicity; and (*c*) the sensitivity of faults to fluid triggering and the evolution of the triggering process. Significant challenges remain in understanding induced seismicity and earthquake triggering mechanisms. Future studies using the data sets collected in recent years, as well as continuing acquisition of data, have the potential both to further advance studies of basic earthquake physics and to improve mitigation efforts for induced seismicity.

Brief Review of Historical Induced Seismicity and Fundamental Early Results

Anthropogenic activities have long been recognized to trigger seismicity. In the 1920s, earthquakes accompanied ground subsidence at the Goose Creek oil field and were attributed to subsurface fluid withdrawal and subsequent reservoir compaction (e.g., Pratt & Johnson 1926). Earthquakes occurred after impoundment of Lake Mead in the 1930s (e.g., Mead & Carder 1941, Carder 1945), and earthquakes related to production and subsidence began in 1936 near the Wilmington field in California (e.g., Segall 1989).

Following these early anthropogenic earthquakes and the acceptance of fluid-related subsurface pressure changes as an earthquake triggering mechanism, some of the most significant early advances in understanding induced seismicity arose from two cases of earthquakes and fluid injection in Colorado in the 1960s. At the Rocky Mountain Arsenal (RMA; e.g., Bardwell 1966, Evans 1966, Healy et al. 1968), disposal of fluid triggered many hundreds of recorded earthquakes, including an M4.8 that occurred approximately 18 months after injection ceased (Herrmann et al. 1981; alternatively estimated as an M > 5.2 by Healy et al. 1968). The M4.8 earthquake at the RMA was the largest known earthquake from fluid injection prior to the recent surge after 2010. At the RMA, the earthquake rate rose and fell in correlation with the injection rate with a short phase lag (∼10 days), though earthquakes continued for years after injection ceased (Healy et al. 1968). Fluid at the RMA was injected into fractured crystalline basement rocks; lower-permeability boundaries slowed pressure dissipation, resulting in protracted seismicity after the cessation of injection (e.g., Hsieh & Bredehoeft 1981). In the second Colorado case in the 1960s, the Rangely oil field (e.g., Raleigh et al. 1976) was used as an experiment in earthquake triggering. Seismicity was intentionally triggered and then modulated by varying the reservoir pressure during water-flooding operations (Raleigh et al. 1976). The seismicity rate rose when subsurface pressure was maintained above a critical pressure threshold and decreased when pressure fell below the estimated
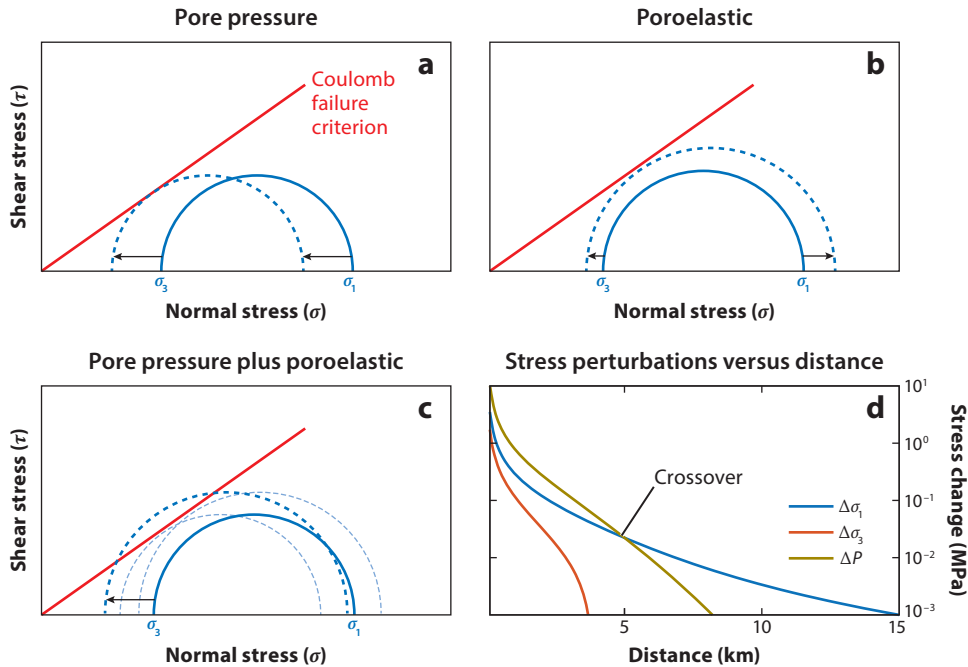
Figure 1

Effects of pore pressure perturbations and poroelastic stress changes on fault failure (schematic). (*a*) Increased pore pressure reduces normal stress on the fault plane, moving the fault closer to the Coulomb failure criterion. (*b*) Poroelastic stresses increase differential stress. (*c*) Combined effects of pore pressure increase and poroelastic stress changes. In panels *a–c*, solid curves represent the initial stress state, and dashed curves represent the perturbed stress state. In panel *c*, light dashed curves are the individual effects from panels *a* and *b*. Pore pressure perturbations and stress changes, as well as the relative magnitude of changes, depend on parameters including time, distance, injection rate, diffusivity, and poroelastic parameters. (*d*) Example calculation of pore pressure and poroelastic stress changes at increasing distance from a well (Rudnicki 1986) using diffusivity of 0.5 m^2/s, injection rate of 0.2 m^3/s, time of 1 year, and a Biot coefficient of 0.5. Pore pressure changes are greater near the well, but poroelastic stress changes are of higher magnitude at greater distance.

critical value. At Rangely, seismicity followed injection within less than a day, indicating rapid pressure transmission along fractures between the injection wells and the main fault (Raleigh et al. 1976). This controlled experiment at Rangely remains one of the best-documented cases of fluid pressure and seismicity rates available in the public domain.

A conceptual model for induced seismicity emerged from these early studies, based upon the model proposed for slip on poorly oriented thrust faults (Hubbert & Rubey 1959). Briefly, fluid pressure within the fault reduces the normal stress resolved on the fault plane and consequently increases the ratio of shear to effective normal stress (e.g., Hsieh & Bredehoeft 1981). This decrease in effective normal stress moves the fault toward the Coulomb failure criterion (**Figure 1a**). Segall (1989) and Segall & Lu (2015) improved this model by including poroelastic coupling between pore pressure and stress, as well as time-dependent earthquake nucleation (**Figure 1b**).

Numerous earthquake sequences following these Colorado earthquakes and preceding the recent surge were also considered to have been induced, though these earthquakes were isolated in space and time. These include the Baldwin Hills, California, injection-related earthquakes (Hamilton & Meehan 1971); the Wilmington, California, extraction-related earthquakes (e.g.,

Kovach 1974); and the M4.3 earthquake triggered in 2000 at the particularly well-monitored fluid injection site in Paradox Valley, western Colorado (Ake et al. 2005, King et al. 2014). Other earthquakes interpreted to be induced include a sequence from 1991 to the present at the Groningen field in the Netherlands (e.g., van Thienen–Visser & Breunese 2015); earthquakes near Ashtabula, Ohio, beginning in 1987 (Seeber & Armbruster 1993, Seeber et al. 2004); and earthquakes near El Dorado, Arkansas, in the 1980s (Cox 1991). These induced earthquake sequences were relatively rare compared to those occurring since 2010 and, other than the notable exceptions described above, were limited to magnitudes below M4.0. For comparison, 79 M > 4.0 earthquakes have occurred within the state of Oklahoma since 2010 [US Geological Survey ANSS Comprehensive Earthquake Catalog (ComCat); **https://earthquake.usgs.gov/data/comcat/**], the majority considered to be induced. In this time period, there have been seven M > 4.0 earthquakes in Texas; four in Colorado, Kansas, and New Mexico, respectively; three in Arkansas; and one in Ohio.

One focus of past studies of induced seismicity was on large-magnitude earthquakes near sites of fluid injection, extraction, or impoundment (e.g., Gupta 1985, Segall 1985, Simpson & Leith 1985). The question of whether these large-magnitude earthquakes were induced was debated (e.g., Segall 1985, Simpson & Leith 1985) and remains controversial (e.g., Ge et al. 2009, Keranen et al. 2013, Walsh & Zoback 2015, Juanes et al. 2016).

Key results from early studies on injection-induced seismicity are as follows:

1. Subsurface pressure changes related to fluid injection are capable of triggering earthquakes.
2. High pore pressure created by fluid injection can reduce normal stress on a fault plane and move a fault closer to the Coulomb failure criterion.
3. Seismicity can occur nearly immediately following injection if the well(s) and faults are linked by transmissive zones (e.g., fractures).
4. Seismicity can occur years after injection ends if pressure does not diffuse to background but remains perturbed locally. Diffusion is inhibited by low-permeability fluid baffles (faults; lateral and vertical lithologic or structural change).
5. A critical pressure threshold exists for rupture on a fault; in the case of Rangely this pressure was estimated to be ∼26 MPa (much higher than critical pressures estimated for recent triggering).
6. Injection-induced earthquakes can reach (at least) moderate magnitudes.
7. Induced seismicity near injection wells is more responsive to variable well parameters such as injection rate; distant remote seismicity occurs (e.g., Paradox Valley) but is less responsive to temporal changes in injection rate.

Induced Seismicity Since 2008: A Rapid Rise in Rate, and a Rapid Rise in Research

A rapid increase in the rate of induced seismicity since 2008, including numerous felt earthquakes and several moderate-sized earthquakes (**Figures 2** and **3**), abruptly raised the impact and public visibility of anthropogenic seismicity. Wastewater disposal well rates and seismicity rates rose after 2008 in Texas, Arkansas, and Oklahoma (e.g., Horton 2012, Ellsworth 2013, Llenos & Michael 2013, Keranen et al. 2014, Frohlich et al. 2016). The rise in induced seismicity included 10 felt earthquakes in late 2008 near the Dallas–Fort Worth airport in Texas (Frohlich et al. 2011). Hundreds of earthquakes, including one of Mw4.7, were recorded near Guy-Greenbrier, Arkansas, from 2009 to 2011 (Horton 2012). In Oklahoma, more than 200 M ≤ 3.9 earthquakes occurred from 2009 to 2011 just ∼20 km east of Oklahoma City (Keranen et al. 2014), and earthquakes were triggered by hydraulic fracturing in southern Oklahoma (Holland 2013a). In Ohio, 109 earthquakes of up to ML4.0 occurred near a deep disposal well near Youngstown in
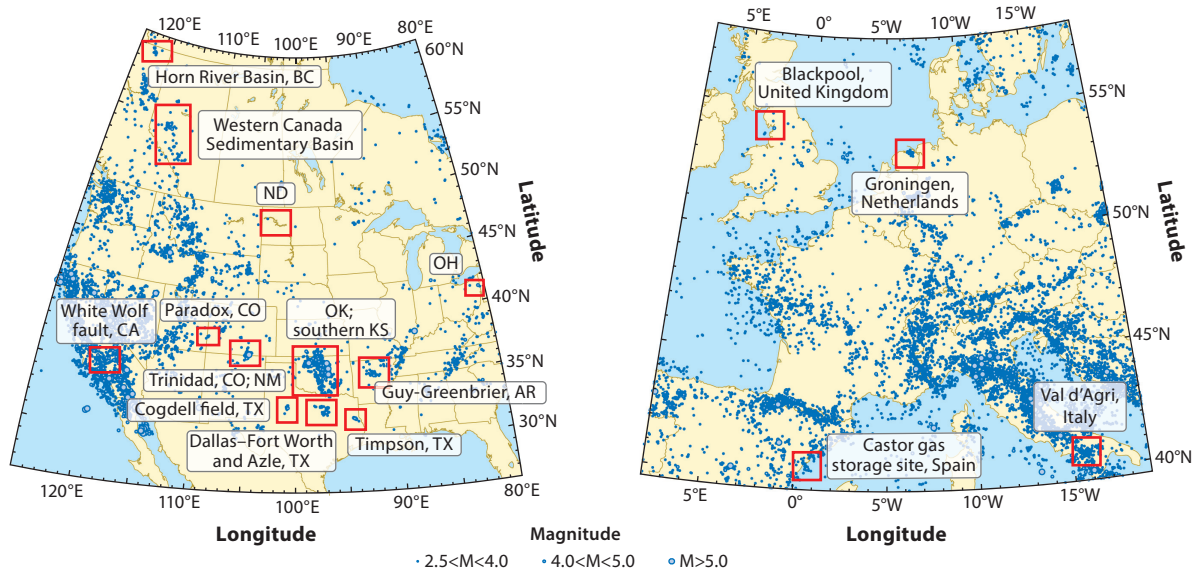
Figure 2

Locations of induced seismicity since 2006 discussed in the text. Earthquake locations and magnitudes are from the US Geological Survey ANSS Comprehensive Earthquake Catalog (ComCat; **https://earthquake.usgs.gov/data/comcat**), the Natural Resources Canada Earthquake Database (**http://www.earthquakescanada.nrcan.gc.ca//stndon/NEDB-BNDS/bull-en.php**), and the International Seismological Centre Catalog (**http://www.isc.ac.uk**). Earthquakes shown for the United States and Canada are M ≥ 2.5 and occurred between January 2008 and June 2017. Earthquakes shown for Europe are M ≥ 2.5 and occurred between January 2006 and June 2017.

2011 (Kim 2013); the largest was felt across northern Ohio. In Canada, a felt ML3.8 earthquake, associated with hydraulic fracturing in the Horn River Basin of British Columbia, was part of a series of earthquakes that occurred locally between 2009 and 2011 (BCOGC 2012, Farahbod et al. 2015). Similarly, an ML2.3 earthquake associated with hydraulic fracturing was felt near Blackpool, United Kingdom, in April 2011 (Clarke et al. 2014, Wilson et al. 2015). Earlier, in Italy, a series of M < 2.2 earthquakes began in 2006 after wastewater disposal in the Val d'Agri field (Valoroso et al. 2009, Stabile et al. 2014). These earthquakes, many of which were felt by local residents, were international in scope and resulted in a sharp increase in the public visibility of induced seismicity related to energy development.

However, the most notable and arguably the most consequential recent induced earthquakes began in 2011, several of which exceeded Mw5.0. These larger earthquakes had a significant impact on motivating an enhanced research focus on induced seismicity. An Mw5.3 earthquake in August 2011 in the region of the 2001 Trinidad, Colorado, earthquakes (Barnhart et al. 2014, Rubinstein et al. 2014) was followed by an Mw5.7 and two Mw5.0 earthquakes near Prague, Oklahoma in November 2011 (Keranen et al. 2013); the Prague earthquakes caused notable damage to local homes, and the Mw5.8 earthquake near Pawnee, Oklahoma, in September 2016 caused changes in local groundwater systems (Manga et al. 2016). Home damage also occurred following shallow earthquakes of up to M3.6 in 2012 in the Groningen field in the Netherlands (van Thienen–Visser & Breunese 2015). Earthquakes associated with the Castor gas storage site offshore Spain reached up to M4.2 in 2013 (Gaite et al. 2016).

Induced earthquakes continue to the present day, resulting predominantly from wastewater disposal, including the Pawnee earthquake in 2016, the largest to date, but also from hydraulic fracturing, including in Ohio (Skoumal et al. 2015b) and in Canada (e.g., Atkinson et al. 2016,
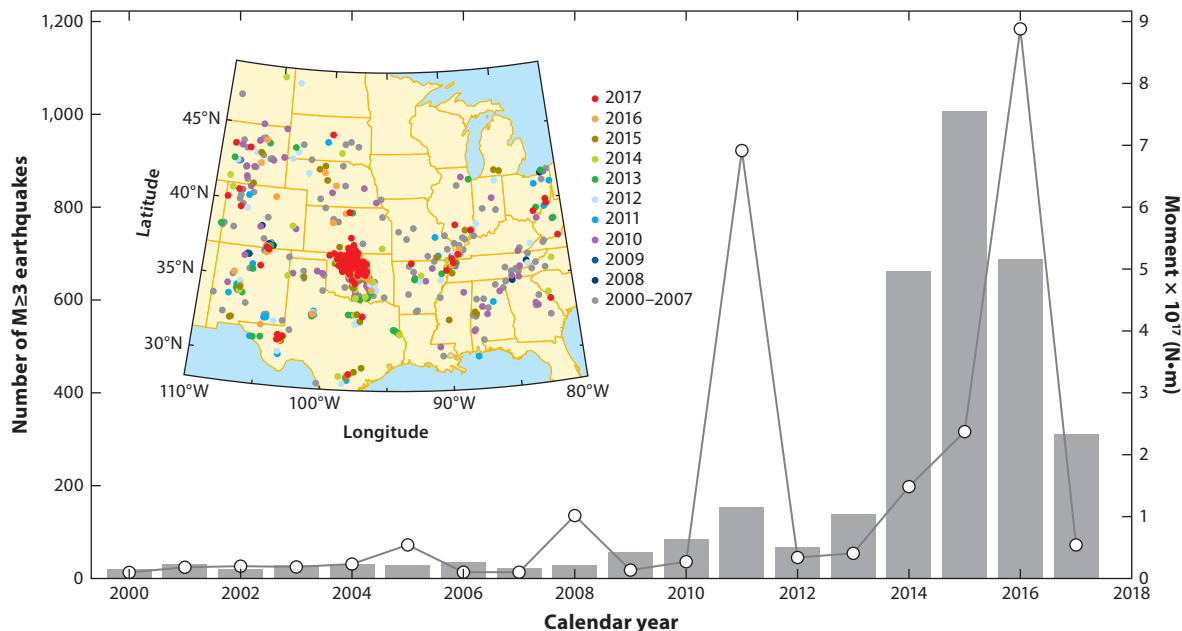
Figure 3

Number of M ≥ 3 earthquakes (*gray bars*) in the central United States from January 2000 to November 2017, along with summed seismic moment release during each year (*white dots*). Inset map shows the locations of the earthquakes from the US Geological Survey ANSS Comprehensive Earthquake Catalog (ComCat; **https://earthquake.usgs.gov/data/comcat**). From 2010 to 2017, the majority of earthquakes have occurred in central and northern Oklahoma. The number of earthquakes peaked in 2015, but total moment release was highest in 2011, when Mw5.7 and Mw5.4 earthquakes occurred in Prague, Oklahoma, and Raton Basin, Colorado, respectively, and in 2016, when Mw5.1, Mw5.8, and M5.0 earthquakes occurred in Fairview, Pawnee, and Cushing, Oklahoma, respectively.

Bao & Eaton 2016). The rate of induced seismicity is far greater in recent years than it was prior to 2000, and these earthquakes are also less isolated spatially, spreading over broad regions and occurring in numerous countries across numerous states within the United States. The rapid surge in induced earthquakes has led to modified regulations for wastewater disposal (Davis & Fisk 2017, Stewart & Ingelson 2017) and has motivated focused studies of quantitative hazard from anthropogenic earthquakes (e.g., Petersen et al. 2016). Along with the regulatory, hazard quantification, and hazard mitigation responses, these recent anthropogenic earthquakes have motivated a strong response from the seismological and hydrogeological research communities.

UNEQUAL DISTRIBUTION OF INDUCED SEISMICITY

A fundamental observation from the last 10 years of seismicity is that induced seismicity is unevenly distributed with respect to fluid injection (e.g., Frohlich et al. 2015, Göbel 2015). The earthquake productivity of a given fluid injection volume varies widely between major basins. At one extreme, the number of induced earthquakes in the Bakken Shale of North Dakota is negligible; nine earthquakes of approximately M > 1.5 were detected over the course of about 2.5 years using the EarthScope Transportable Array, with a maximum magnitude of 2.6 (e.g., Frohlich et al. 2015). Two earthquakes are in ComCat for North Dakota since 2008; the larger one was an M3.3 in 2012. Texas, Colorado, and California have experienced induced earthquakes, but in relatively isolated regions and apparently related to a restricted number of wells (e.g., Weingarten et al.

2015, Goebel et al. 2016, Hornbach et al. 2016). On the other extreme, the state of Oklahoma has experienced over 2,500 M3.0 earthquakes and over 9,000 M1.5 earthquakes between 2008 and 2017, the majority of which were likely induced, including five M ≥ 5.0 earthquakes to date (ComCat). Although Oklahoma wells have high injection volumes (e.g., Keranen et al. 2014, Walsh & Zoback 2015), wells in other states, such as Texas, also operate at high rates (Hornbach et al. 2016) but have not produced comparably sized regions of seismicity or amounts of moment release.

Fault-Scale Variations in Seismicity

Within each region of induced seismicity, earthquakes vary widely in distribution. The most specific variability in distribution is manifested by the isolation of earthquakes onto narrow fault planes (e.g., Goertz-Allmann et al. 2017, Lambert 2017, Schoenball & Ellsworth 2017). At the spatially isolated extreme of cases of induced seismicity, an isolated sequence of earthquakes occurs in close proximity to a well or wells, as occurred in the Rangely case. The isolation onto a fault plane is caused by direct pressure transmission between the well(s) and a fault (e.g., Raleigh et al. 1976). At the spatially broad extreme of cases of induced seismicity, pressure transmission between wells and faults likely follows a tortuous path through zones of high permeability. Pressure perturbations from large wells or sets of wells, in regions of high permeability, can reach tens of kilometers from the wells (Keranen et al. 2014, King et al. 2014, Mulargia & Bizzarri 2014, Yeck et al. 2016). However, even in these cases, where seismicity occurs over a broad region, a similar crisp delineation of faults and nonseismic regions is still ubiquitously observed (**Figure 4b**). The pressure perturbations presumably propagate between seismically active faults without triggering detectable seismicity. These aseismic pathways may consist of poorly oriented fault and fracture sets; well-oriented seismic lineations in Oklahoma are offset from one another along the trend of these poorly oriented fractures (Liu et al. 1991), which appear to be serving as fluid pathways (Lambert 2017), similar to what is observed in Paradox Valley (King et al. 2014). Both well-oriented and poorly oriented fractures transmit fluid in these cases, unlike in other regions, where fluids are found primarily within critically stressed faults (Townend & Zoback 2000).

Regional-Scale Variations in Seismicity

At a regional scale, the seismic moment release varies spatially across geological structures and between basins. The dual observations that earthquakes occur far from wells yet are elsewhere limited to sharp boundaries (**Figure 4a,b**) require rapid lateral variability in permeability or stress state. High bulk permeability, likely within fracture systems in sediment or basement, is necessary for the distant impacts of fluid injection. The sharp boundaries of seismicity correlate to large fault systems that appear to effectively create permeability baffles and limit the spatial extent of seismicity (Lambert 2017). Stratigraphic transitions can also limit pressure propagation; for example, seismicity is contained within carbonate reefs at the Cogdell field near Snyder, Texas (Davis & Pennington 1989), and concentrates along the edges of reefs in Alberta, Canada (Schultz et al. 2016).

GEOLOGICAL CONTROLS ON INDUCED SEISMICITY: HYDROGEOLOGICAL MODELING

The geological factors of lithology, layering, cementation, and fractures create lateral and vertical permeability variations and are the dominant control on variability in induced seismicity. These permeability variations regulate the subsurface fluid pressure field (in time and space) that results from a given volume of injection and also control the volume of fluid that can be injected without exceeding a given pressure threshold. In a region of high isotropic bulk permeability,
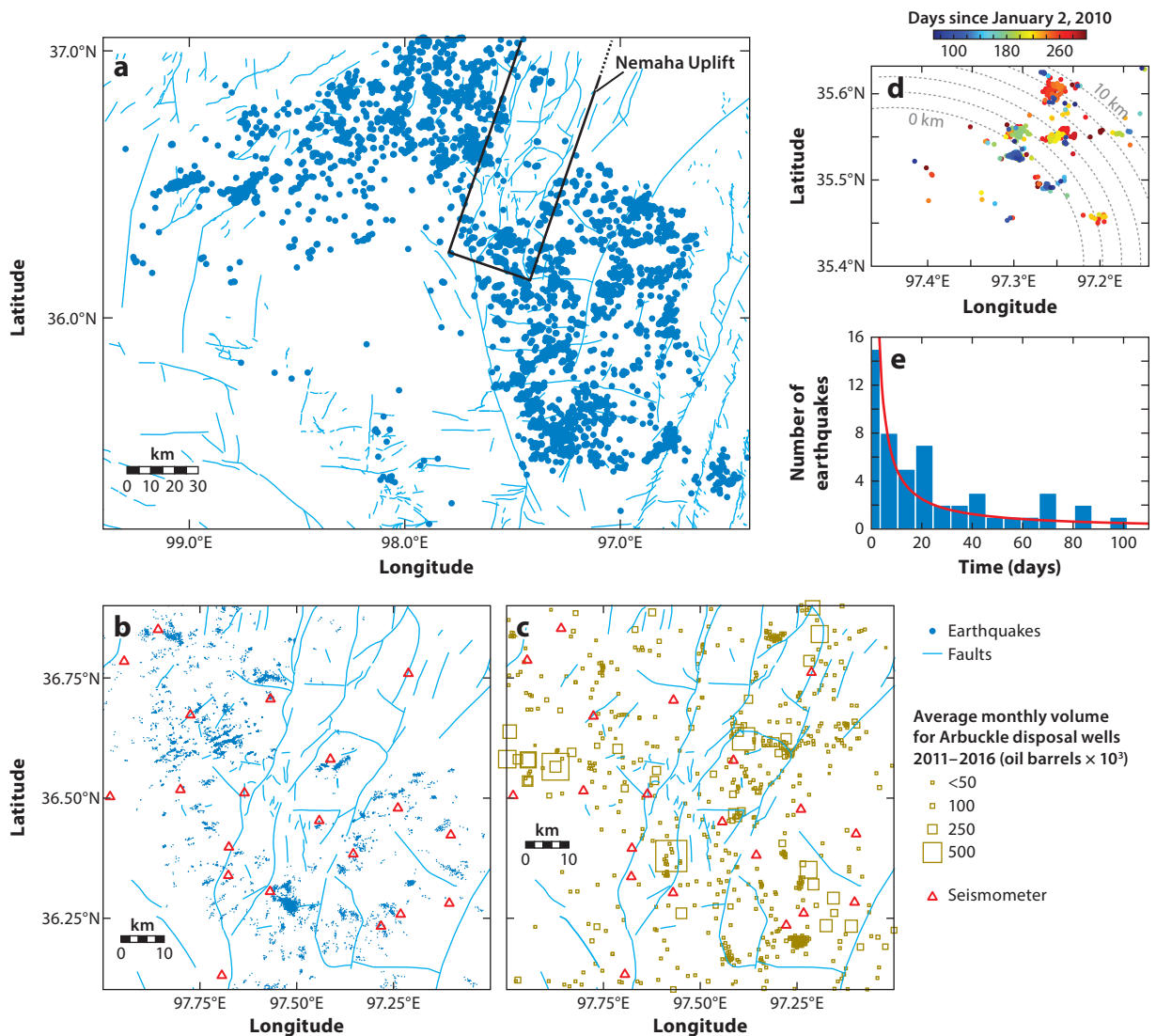
Figure 4

(*a*) Earthquakes and faults in northern Oklahoma, 2009–2016. Shown are M ≥ 2.5 earthquakes from the US Geological Survey ANSS Comprehensive Earthquake Catalog (ComCat; **https://earthquake.usgs.gov/data/comcat**). Earthquakes are spread over a broad region but are sharply bound laterally by large faults. Faults in panels *a*–*c* are from Marsh & Holland (2016). (*b*) Earthquakes in north-central Oklahoma from a local catalog (Lambert 2017) delineate discrete fault planes but rarely coincide with mapped faults. Seismic instruments (*red triangles*) include stations from Cornell University, the US Geological Survey, the Oklahoma Geological Survey, and Oklahoma State University (see Lambert 2017). (*c*) Disposal wells in north-central Oklahoma [Lambert 2017; data from the Oklahoma Corporation Commission (**http://www.occeweb.com/og/ogdatafiles2.htm**)]. Earthquakes are unevenly distributed with respect to volume of injected fluid and are nearly absent around wells within the Nemaha Uplift. (*d*) Lateral migration of seismicity in the Jones swarm (modified from Keranen et al. 2014). Earthquakes occurred on individual planes with a northeast spatial migration through time. (*e*) Omori-type decay of seismicity for earthquakes following an M4 earthquake in north-central Oklahoma. Earthquakes in north-central Oklahoma exhibit a combination of this Omori-type mainshock-aftershock behavior and swarmlike behavior.

pore fluid pressure variations diffuse rapidly away from an injection point. In a region of low bulk permeability, pressure diffuses slowly for the equivalent volume of injected fluid.

Two-dimensional radial models of fluid flow in a confined layer demonstrate these basic concepts (**Figure 5d–f**). Though the models presented here are purely of pore pressure effects without poroelastic effects (e.g., Segall & Lu 2015), they provide basic insight into the relative effects of flow rate and permeability on reservoir pressure effects. The models use MODFLOW (Harbaugh et al. 2017) and representative values for hydrogeological parameters, injection reservoir thickness, and injection rates:

- Model A1. High permeability and high flow rate (1,000,000 barrels/month), approximating the largest disposal wells.
- Model A2. Moderate permeability and moderate flow rate (250,000 barrels/month), similar to average north-central Oklahoma wells.
- Model A3. High permeability and low to moderate flow rate (150,000 barrels/month), similar to North Dakota wells.

Two additional models (**Figure 5b,c**) add complexities to the above models, including the effects of multiple active wells within a region and of lateral permeability changes:

- Model B1. Model A2 with multiple wells at 5-km spacing.
- Model B2. Model A3 with a lower-permeability structure to represent lateral permeability change, either stratigraphic or fault related.

Models A1 and A2 use values of hydraulic conductivity from recent measurements in Oklahoma (Carrell 2014, Perilla Castillo 2017), indicating permeability from hundreds to thousands of millidarcys. Disposal rates are representative of wells active in the state. Model A3 uses hydraulic conductivity estimates from the Dakota Group in North and South Dakota (Rahn 2014, Bader 2017) and flow rates from the larger North Dakota wells (Bader 2017). All models use a 60-m-thick disposal unit, based on thicknesses of the Inyan Kara member of the Dakota sandstone unit (e.g., Bader 2017).

The suite of models (**Figure 5**) highlights the combined influence of geological variability (permeability) and flow rate. The high-permeability, high–flow rate model (A1) creates the largest area of perturbed reservoir, with relatively low near-wellbore pressures. In the moderate-permeability model (A2), pressures are higher near the wellbore but affect a relatively smaller volume. The high-permeability and lower–flow rate model (A3) results in lower pressure throughout the reservoir, both near-field and far-field. With multiple wells (B1), pressure fronts superimpose. Pressure builds slowly over time in the model with a lateral decrease in permeability (B2), reaching critical pressures over 10 years after injection began. Critical pressure in the subsurface can be attained near or far from the wellbore, with short or long time delays from the onset of injection, depending upon injection rate and permeability structure.

Spatial variations in pore pressure on the order observed in the models would impact the distribution of seismicity. Though faults triggered by induced seismicity are commonly unmapped prior to rupture, statistical models can provide estimates of probable distributions. Faults commonly follow a power-law model for the distribution of fault length (e.g., Yielding et al. 1996), and an exponent of −1.5 roughly predicts one 10-km-long fault, approximately three hundred 1-km-long faults, and approximately one thousand 100-m-long faults within our modeled area. A 10-km-long fault is potentially capable of hosting an M6 earthquake (Wells & Coppersmith 1994), and the 1-km-long and 100-m-long faults are ruptures of approximately M4 and M3, respectively (Abercrombie 1995).

These results qualitatively match observations of infrequent triggering of M > 5.0 induced seismicity; no large faults are encountered in most simulations because of the relative paucity of
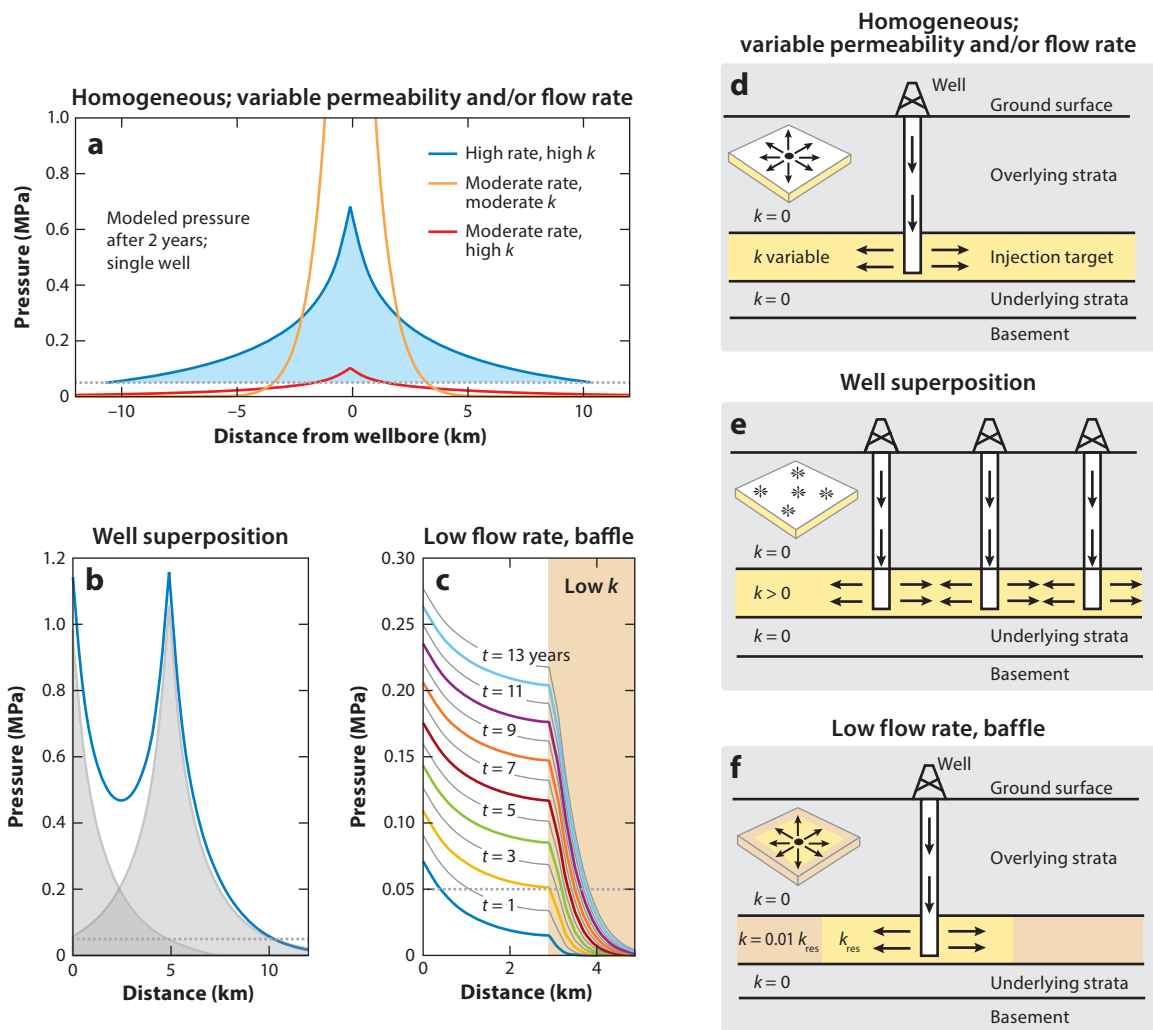
Figure 5

Conceptual hydrogeological models of pore fluid pressure variations calculated using MODFLOW (Harbaugh et al. 2017). Poroelastic effects are not included in these conceptual models. (*a*) Models of pore fluid pressure perturbation following injection at a single disposal well, parameterized with high flow rate and high permeability (*blue*); moderate flow rate and moderate permeability (*yellow*); and low to moderate flow rate and high permeability (*red*). The gray dashed lines in panels *a–c* represent a failure threshold of 0.05 MPa. The shaded blue region represents the area above the failure threshold for the high–flow rate and high–injection volume scenario. (*b*) Superposition of pore pressure perturbations from moderate-rate wells at 5-km spacing (*blue line*). The shaded gray region indicates the pressure around each individual well in isolation. (*c*) Pore pressure perturbation in a region with low flow rate (25,000 barrels/month) and a lateral 100-fold decrease in permeability at 3 km from the wellbore, representing stratigraphic or structural change. Pressure builds slowly within the reservoir; critical pressure thresholds can be surpassed without high bottomhole pressure for low flow rates and reasonable reservoir parameters. (*d–f*) Conceptual models for the scenarios in panels *a–c*, respectively. Abbreviations: k, permeability; k_{res}, the permeability of a hypothetical, laterally restricted reservoir.

large faults and the volume of perturbed subsurface pressure. However, a combination of high rate and high permeability increases the probability of the critical pressure threshold encountering such a fault. The pressure near the wellbore was highest for moderate-rate wells in moderate-permeability strata, but the perturbation extended to a lesser distance. Thus, probabilistically, the pressure increase for moderate wells will encounter fewer faults but may trigger faults with a wider range of orientations and thus have a higher probability of triggering faults near the wellbore. In models with lower injection rates in high-permeability strata (similar to what is found in North Dakota), high pressure encounters very few faults; the area perturbed above the 0.05-MPa threshold is restricted to within ~1 km of the wellbore (**Figure 5a**). For low injection rates, earthquakes would be expected to be rare and would occur only very near the wellbore if faults are present. This dependence upon injection rate assumes that wells are randomly distributed. In practice, however, wells are more common near large faults because of the increased abundance of structural traps, which increases the likelihood of larger earthquakes beyond the number expected in random probabilistic models.

The concentration of large injection-induced earthquakes in recent years within Oklahoma is consistent with the results that high-rate injection into zones of high permeability may result in the greatest potential for larger earthquakes.

The models provide simple conceptual insight into the impacts of injection scenarios on seismicity. No poroelastic effects are included, the pressure threshold used is an estimate that may change for each region and fault, and the power-law distribution of faults is a generic attempt to characterize fault-size variability below the scale at which faults are reliably mapped. Additionally, the hydrogeological modeling is greatly simplified; the model does not include anisotropy and uses constant values within the layer for hydrogeological parameters. The upper and lower boundaries of the injection unit have zero permeability, rather than the low (but nonzero) permeability that would be expected if it were bounded by shale-rich layers, or the high permeability that would be expected if it were sitting above fractured basement.

GEOLOGICAL IMPACTS: CASE STUDIES OF THE EFFECTS OF INJECTION RATE AND LOCAL GEOLOGY

The question of why some regions do not have induced earthquakes is of great importance both for mitigation and for understanding the process of earthquake triggering. These regions may have insufficient rates or volumes of fluid injection to increase pore pressures beyond critical levels (e.g., Frohlich et al. 2015), particularly with respect to the permeability of the disposal units (**Figure 5a**). Alternatively, vertical barriers to pressure transmission into basement—for example, the barrier posed by the presence of a low-permeability basal sedimentary layer—are proposed to inhibit triggering by preventing pressures from reaching basement faults (e.g., Zhang et al. 2013).

North Dakota: Little Seismicity from Moderate Injection Rates

A notable case of moderately high-rate disposal (e.g., ~150,000 barrels/month) with few earthquakes is the Williston Basin in North Dakota and Canada (e.g., Frohlich et al. 2015). In North Dakota, disposal is dominantly targeted at the Dakota formation, which has permeability and hydraulic conductivity values similar to or higher than those estimated for the Arbuckle formation in Oklahoma (Rahn 2014, Bader 2017). However, this formation is confined above and below by low-permeability sedimentary strata and is located high in the sedimentary section relative to basement (Murphy et al. 2009). Fluid pressure thus likely has few direct pathways to basement, unlike in Oklahoma, where the target Arbuckle formation commonly lies directly above basement

or is separated by a thin sandstone. Many wells in Oklahoma also initially disposed directly into Precambrian basement. The low rate of seismicity in North Dakota likely results from a combination of (*a*) low subsurface pressures regulated by injection rate and permeability and (*b*) the geological isolation of the disposal unit. Similarly, wells in other areas where injection targets are at levels far above basement, such as southern Oklahoma, do not result in significant seismicity.

Swan Hills, Alberta, Canada: Seismicity Induced at Low Injection Rates

Low rates alone are insufficient safeguards against induced seismicity, as seen in the Swan Hills field in Alberta, Canada (Schultz et al. 2016). Wells operate at rates of 25,000 barrels/month, far lower than the rate of 300,000 barrels/month noted by Weingarten et al. (2015) as the threshold over which induced seismicity becomes more likely. Schultz et al. (2016) suggested instead that the local geology rapidly transfers fluids to basement: Reefs may have nucleated on the basement faults, providing nearby earthquake sources and rapid fluid communication. Alternatively, lateral permeability changes at the reef margins may raise pressure, particularly because the earthquakes are observed to cluster at the margins of the reefs. Regardless, these earthquakes near low-rate wells indicate that rate and volume alone are insufficient parameters to predict or avoid induced seismicity, which responds to the combination of permeability structure and injected volume.

VARIABILITY IN STRESS STATE

The background tectonic stress field could also contribute to the observed variability in induced seismicity (e.g., King et al. 2014, Göbel 2015). If faults in a region are not near critical failure because of the principal stress magnitudes, small pressure perturbations would be insufficient to trigger slip, as proposed for the Auburn Geothermal Well in New York (Hickman et al. 1985) and in the Newark Basin (Zakharova & Goldberg 2014). However, stress magnitude data are relatively rare in the public domain (Heidbach et al. 2010) and are not sufficient for full analyses of links between stress state variability and induced seismicity. Van der Elst et al. (2013) instead attempted to use the triggerability of a fault to estimate the fault proximity to failure. The results from this study intriguingly suggest that faults near failure could potentially be identified by high rates of dynamic triggering; systematic characterization of triggerability could theoretically map regions with and without critically stressed faults and provide a crude proxy for the relative principal stress magnitudes. Further tests of this method remain a future research direction.

MAXIMUM MAGNITUDE AND RELEASE OF TECTONIC STRAIN

The maximum magnitude of an induced earthquake is debated (e.g., McGarr 2014, Atkinson et al. 2016, van der Elst et al. 2016). One possible upper bound is the largest natural earthquake that could occur in the given region (van der Elst et al. 2016). Another bound is an upper limit proportional to the volume of fluid injected, for example, equal to the volume of fluid injected times the modulus of rigidity (McGarr 2014). Induced earthquakes appear capable of near-field triggering of other earthquakes via stress transfer (e.g., Keranen et al. 2013, Sumy et al. 2014), as seen in the Prague, Oklahoma, earthquake sequence in 2011, similar to triggering of near-field sequences following natural earthquakes (e.g., Gomberg et al. 1998, Stein 1999). In Prague, the main Mw5.7 rupture was moved close to failure by static Coulomb stress changes following the first earthquake (Sumy et al. 2014), and the faults ruptured progressively to the south as the sequence progressed (Keranen et al. 2013). The correlation observed by McGarr (2014) is dependent upon the area used in the analysis; earthquakes such as the Fairview, Oklahoma, Mw5.0 (Yeck et al. 2016) and others in

Canada (Atkinson et al. 2016) provide counterexamples in which the volume of fluid injected near the faults is lower than expected by the McGarr (2014) model. The individual earthquake rupture size resulting from fluid triggering is not well understood, however, nor are earthquake magnitudes in purely tectonic cases (e.g., Olson & Allen 2005, Rydelek & Horiuchi 2006).

NEW KNOWLEDGE OF STRUCTURE AND EARTHQUAKE PHYSICS

Tying Together Slip Processes Observed in Controlled and Natural Settings

Induced seismicity is also being used intentionally in natural field settings to study earthquake mechanics. These controlled experiments, while few in number, allow detailed data acquisition during earthquake nucleation on faults with realistic frictional properties, geometry, and state variables. The field experiments thus serve as a bridge between smaller-scale laboratory experiments on typically planar faults with homogeneous material properties and fortuitous observations of natural earthquakes. In a shallow experiment in carbonates, controlled fluid injection into a small-offset fault zone triggered dominantly aseismic slip in the zone pressurized by injected fluid, along with a 20-fold increase in permeability (Guglielmi et al. 2015). The aseismic slip process triggered by the fluid pressurization in turn triggered microseismicity of magnitude less than -2, interpreted to likely occur off of the main fault/pressurized zone within the surrounding damaged rock as an indirect effect of the aseismic fault slip (Guglielmi et al. 2015). Results similar to those from Guglielmi et al.'s (2015) experiment have been observed in unintentional field experiments; aseismic slip may have driven aftershocks of the 2011 Mw5.7 Prague, Oklahoma, earthquake on a previously aseismic intersecting fault plane near the southern end of the rupture area (Savage et al. 2017a). Aftershocks on this fault were initially distributed within a zone ~150 m wide and localized onto the fault plane prior to an Mw5.0 earthquake in the region of localization. Aseismic slip, triggered by coseismic fluid pressure propagation or by coseismic static stress transfer, appears to have triggered aftershocks on small faults within the damage zone of the intersecting and nearly orthogonal fault plane, leading eventually to the nucleation of the Mw5.0 on the main fault plane (Savage et al. 2017a). Such a model supports models of the preslip process for earthquake nucleation (e.g., Ellsworth & Beroza 1995).

Because earthquakes are not necessarily self-similar over magnitude scales, small earthquakes may not fail via the same processes as larger earthquakes (e.g., Viesca & Garagash 2015). A proposed project, Scientific Exploration of Induced SeisMicity and Stress (SEISMS; Savage et al. 2017b), thus proposes to use fluid pressure to induce a moderate-sized earthquake on a well-instrumented natural fault to probe the physical causes of earthquake slip and arrest. Similar to the 1960s Rangely experiment, these natural experiments provide a measure of control on subsurface pressure perturbations along a known fault, facilitating high-frequency and dense monitoring of the earthquake rupture process.

Laboratory rock mechanics experiments are also now beginning to include fluid in earthquake nucleation to characterize frictional properties and velocity-strengthening versus velocity-weakening behavior in the presence of fluids (e.g., Scuderi & Collettini 2016). These experiments have the potential to provide insight into, among other results, the role of fluid pressure in promoting stable sliding versus unstable behavior.

Induced Earthquakes as a Model System for Natural Earthquakes

Though induced earthquakes could theoretically have rupture mechanisms different from those of natural earthquakes, numerous observations from natural earthquakes suggest that fluids are

commonly involved. The Hubbert & Rubey (1959) hypothesis for thrust faulting was the initial model for induced seismicity. Fluids are ubiquitous along subduction zone megathrusts (Saffer & Tobin 2011) and are common in other faulting styles (Sibson 1992, 2000). Gold mineralization indicates high fluid pressure in earthquakes (Weatherley & Henley 2013). Dehydration under the given pressure-temperature conditions at natural seismogenic depths releases fluids along faults (Connolly 1997, Hacker 1997). Slow slip and tremor on both megathrusts and strike-slip faults are widely considered to be fluid related (Liu & Rice 2007). Across wide ranges of tectonic regimes, fluid is intimately involved in fault zone and earthquake processes, and insights gained from studies of anthropogenic fluid-triggered seismicity are relevant to studies of natural fault systems. The pervasive distribution and frequency of induced earthquakes have effectually created a large-scale, systematic experiment in earthquake triggering and fluid-fault processes. Similar to the advantages fruit flies provide for genetic research (e.g., Beller & Oliver 2006), the current profusion of induced earthquakes within an anticipatable region provides a tool for studies of earthquake process.

Fault Orientation: Failure of Both Critically Stressed and Suboptimal Faults

Earthquakes in Oklahoma largely occur on faults that are well oriented in the background stress state (Holland 2013b, Alt & Zoback 2016, Lambert 2017), though rupture does also occur on poorly oriented faults. In northern Oklahoma, faults defined by earthquake ruptures are well oriented and underlie larger, aseismic, mapped faults ~20° from an optimal orientation (**Figure 4b**) (Lambert 2017), indicating that well-oriented faults or fractures are pervasively present throughout crystalline basement. The Pawnee earthquake sequence ruptured well-oriented faults, and the larger mainshock of the Prague earthquake sequence (Mw5.7) was optimally oriented (Keranen et al. 2013, Sumy et al. 2014). However, other ruptures occurred on suboptimal orientations: At Rangely, the rupturing fault was suboptimally oriented and required over 25 MPa of downhole pressure for the fault to slip (Raleigh et al. 1976). Suboptimal faults near the Paradox Valley disposal well ruptured; the injection operated at up to ~80 MPa downhole pressure (Ake et al. 2005). The initial Mw5.0 Prague mainshock ruptured at ~30–40° [the Global CMT catalog (Ekström et al. 2012) estimates a 27° fault plane; the most northern aftershocks trend at 40° in the relocated catalog] (**Figure 6**) and triggered the subsequent, larger Mw5.7 on the more optimally oriented intersecting fault (Keranen et al. 2013). Fluid pressure increases in the subsurface in regions of lateral permeability variations (Keranen et al. 2013, King et al. 2014) increase the range of triggerable fault orientations, allowing suboptimal faults to fail.

Hidden Faults

Most faults that rupture in Oklahoma are unmapped, occurring both on fractures and small faults in basement (**Figure 4b**) and on larger faults, as in the cases of the Prague Mw5.7 and the Pawnee Mw5.8 earthquakes. The common rupture of unmapped faults underscores that the orientation of mapped faults is not sufficient to characterize induced seismic hazard, even in conjunction with hydrogeological modeling.

CHALLENGES IN INDUCED SEISMICITY: TECTONIC VERSUS INDUCED EARTHQUAKES

Much of the effort in the field of induced seismicity has been focused on determining a method to distinguish definitively between induced and natural earthquakes. Statistical metrics have long been used (e.g., Davis & Frohlich 1993) and remain frequently employed; they focus primarily
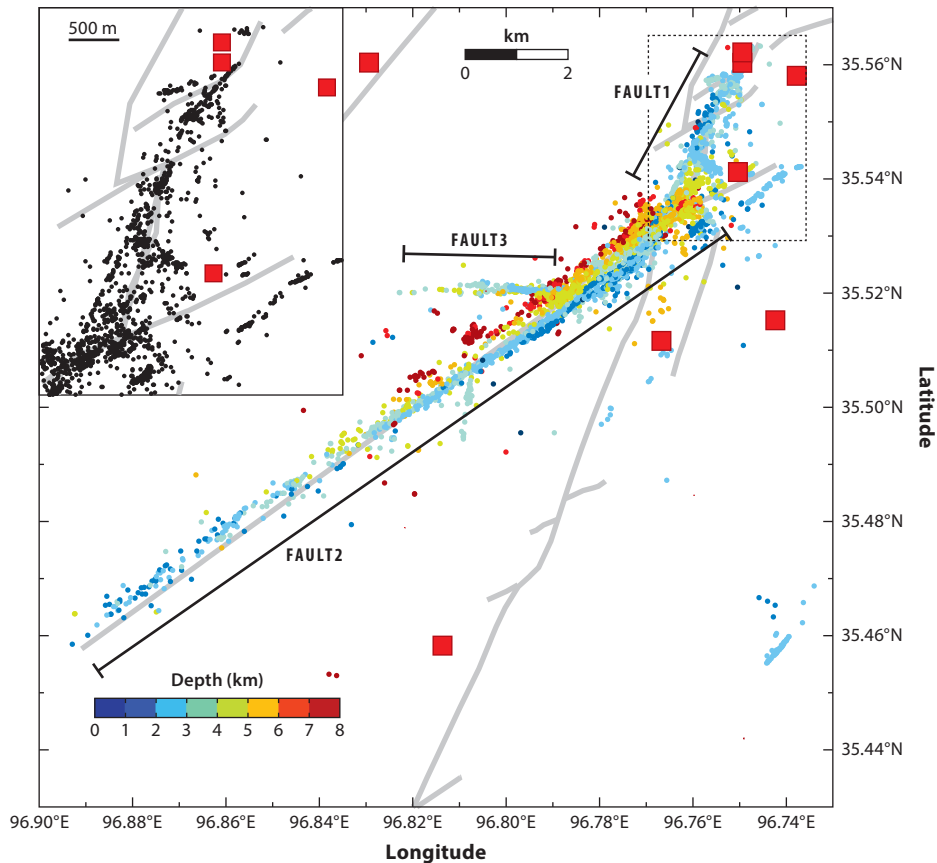
Figure 6

Earthquakes recorded during the 2011 Prague, Oklahoma, earthquake sequence. FAULT1: Mw5.0 on November 5. FAULT2: Mw5.7 on November 6. FAULT3: Mw5.0 on November 8. A larger scale of the dashed box near the initial hypocenter is shown in the inset. Earthquakes occurred within the Wilzetta Fault Zone (*gray lines*; Marsh & Holland 2016). (*Inset*) Zoom of earthquakes near the initiation point of the sequence. The first rupture plane was not optimally oriented; the second, largest rupture plane was near optimal orientation; and the third rupture plane was poorly oriented (e.g., Sumy et al. 2014). Red squares indicate disposal wells [data are from the Oklahoma Corporation Commission (**http://www.occeweb.com/og/ogdatafiles2.htm**)].

on the distance of earthquakes from injection wells and temporal correlations to injection, as well as on deviations from historical seismicity. Recent studies have attempted to distinguish induced earthquakes using characteristics of the earthquake source, including earthquake stress drop (e.g., Sumy et al. 2017); swarm behavior, or b-value (e.g., Goebel et al. 2016, Skoumal et al. 2016); and ground motion attenuation (e.g., Hough 2014, Yenier et al. 2017). Here we discuss each of these approaches.

Spatial Patterns: Earthquakes Can Occur at Great Distances from Wells

Criteria used for identifying induced earthquakes (Davis & Frohlich 1993, Weingarten et al. 2015) often rely heavily upon spatial correlations between wells and earthquakes. However, the recent

earthquakes have demonstrated that the spatial extent of induced seismicity is widely variable. Induced earthquakes occur near wells but also at much greater distances (Keranen et al. 2014, King et al. 2014, Yeck et al. 2016). Recent earthquakes have also indicated that faults and fractures between basement and disposal units can transmit pressure pulses downward, triggering earthquakes kilometers below injection levels (e.g., Rubinstein et al. 2014). Temporally, earthquakes are observed to migrate spatially for fluid-related earthquakes (**Figure 4d**) (Keranen et al. 2014), but with the number of wells in Oklahoma injecting together currently, clear spatial patterns are unusual at detectable levels. However, migration is not entirely absent. It is observed along individual faults where the numbers of injection wells and earthquakes are low. Detection of the migration along such faults requires a catalog with a low detection threshold that uses local stations; the pattern is not observed in ComCat.

Temporal Correlations: Induced Earthquakes at Short, Moderate, and Long Time Delays

Earthquakes can be triggered with variable time delays, depending upon the well and fault locations and pressure pathways. In areas of hydraulic fracturing and geothermally induced earthquakes, earthquake sequences often exhibit a short-term temporal correlation with injection (e.g., Majer et al. 2007, Holland 2013a, Skoumal et al. 2015b). For a small volume injection, the region of perturbed fluid pressure is small, and little time delay occurs between injection and earthquakes. Cases where known fault conduits exist between the wells and the fault also show rapid triggering (e.g., Rangely; Raleigh et al. 1976). Earthquakes occurring following moderate or long time delays, with little temporal correlation to injection parameters, occur where stratigraphy or faults delay pressure dissipation. At the RMA, earthquakes were initially correlated with injection but continued ~2 years after injection. Injection at the RMA occurred within a fracture zone surrounded by less-permeable crystalline basement (Hsieh & Bredehoeft 1981). Earthquakes were triggered after 18 years in the Cogdell field in Texas, where fluid injection occurred within a reef complex in a stratigraphic trap, i.e., where lateral lithologic changes inhibit fluid pressure diffusion (Davis & Pennington 1989).

Keranen et al. (2013) argued that long-term injection triggered the 2011 earthquake sequence near Prague, Oklahoma. Though McGarr (2014) focused on more recent, higher-rate wells, injection occurred into sedimentary units inside of a faulted network (**Figure 6**), and both long-term and recent wells feasibly contributed. Faults are well known to act either as significant baffles to fluid flow or as fluid conduits (e.g., Smalley & Muggeridge 2010, King et al. 2014, Wibberley et al. 2017). When faults are baffles, the structures strongly inhibit the equalization of fluid pressure (Wibberley et al. 2017). The 27–40° orientation of the initial Mw5.0 fault plane in the Prague sequence is consistent with triggering at a higher pressure; the fault was not critically stressed in the background stress field (**Figure 6**). In a stress field with the maximum horizontal stress at an orientation of N80E (Sumy et al. 2014), with the intermediate stress the overburden pressure, and with well-oriented faults at critical failure, >2 MPa of pressure would have been required for rupture.

The variable time delays observed for the onset of seismicity are caused by geological variability. Each fault requires a critical pressure change to reach failure; multiple combinations of injection rate, pressure, and permeability structure can produce those pressure changes. For wells in hydraulic communication with a nearby fault, earthquakes can occur rapidly following injection (hours to days). For wells in zones of high bulk permeability, earthquakes can occur at great distance from wells with a time delay related to the speed of pressure propagation (approximately months), and for wells in regions with strong lateral permeability changes, fluid pressure can build

up over long time periods (years to decades). Because of large variability in the geological characteristics of oil fields, large variability should be the expectation for the timing of induced seismicity and the distance to wells.

Statistical Discrimination of Induced Seismicity

Regional statistics are often employed to evaluate the likelihood of induced versus tectonic earthquakes for groups of earthquakes occurring over large areas (e.g., Llenos & Michael 2013). For the central United States, Llenos & Michael (2013) determined that the rate of seismicity deviated from background rates in Oklahoma and Arkansas in 2009. Rates in Western Canada deviated from background rates in 2010 (Atkinson et al. 2016). Walsh & Zoback (2015) analyzed statistics within smaller regions in Oklahoma, and within one microregion around the 2011 Prague earthquakes. In the primary regions, increased injection rates preceded increased seismicity (e.g., Keranen et al. 2014). The small box used around the Prague earthquakes deviated from the pattern observed elsewhere (Walsh & Zoback 2015). However, small subsets of the other regions showed results similar to the Prague subset, indicating that regional statistical correlations are not robust in small regions. The Fairview, Oklahoma, Mw5.0 earthquake in 2016 also occurred in a region of low fluid injection (Yeck et al. 2016) but is broadly considered induced. The Prague sequence has not been shown to differ from the other recent Oklahoma earthquakes and is as likely as the other Oklahoma earthquakes to be induced.

Seismological Discrimination of Induced Seismicity

Fluid-related earthquakes are observed in volcanic settings, often in swarms (e.g., Shelly et al. 2013), with b-values that differ from tectonic values. Attempts have been made to apply a similar expectation of swarm behavior to induced seismicity (e.g., Skoumal et al. 2015a, 2016). However, induced seismicity in the past 10 years has occurred in both swarmlike and mainshock-aftershock styles of behavior, without a strong bias toward one or the other. The Fairview Mw5.0 earthquake and the Pawnee Mw5.8 earthquake are broadly considered induced (e.g., Yeck et al. 2016), yet they demonstrated clear mainshock-aftershock sequences. Smaller earthquakes in Oklahoma also frequently occur in mainshock-aftershock Omori-type decay sequences (e.g., **Figure 4e**), and a measure of swarminess is not able to discriminate induced earthquakes reliably. There has been evidence presented for low stress drop for induced earthquakes, by using earthquake spectra (Sumy et al. 2017) and by comparing the rupture area for induced earthquakes to the seismic moment (e.g., Barnhart et al. 2014); however, other studies have indicated that stress drops are on the order of those from tectonic earthquakes (Huang et al. 2016). Ground attenuation is suggested to be lower for induced earthquakes in the central United States (Hough 2014); however, the difference in ground motion can simply be the result of the shallow focal depth of these earthquakes (Atkinson 2015). Though multiple methods have been proposed, no seismic method is clearly capable of discriminating between induced and natural earthquakes, and there is no evidence that induced earthquakes are inherently different from natural earthquakes.

Discrimination of Induced Seismicity in Tectonically Active Regions

In regions of abundant natural seismicity, as in the case of oil fields in California near the San Andreas fault, there is an even greater challenge in distinguishing between natural and anthropogenic causes of earthquakes. For an earthquake swarm with three M > 4 earthquakes near the White Wolf fault, Goebel et al. (2016) modeled pressure changes from wastewater injection and

concluded that pressure increases were enough to trigger the seismicity and that the swarm exhibited classic migration patterns, potentially low b-values, and a temporal correlation to injection. Goebel et al. (2016) concluded that induced seismicity in California would elude detection without detailed seismological, geological, and hydrogeological analyses. Discriminating induced seismicity in active tectonic regions will be a substantial challenge, but an early awareness of induced seismicity occurring near active faults would allow for prompt mitigation.

Reevaluation of Past Earthquakes as Possibly Induced

Results from the recent advances in understanding induced seismicity have been used to reevaluate possible triggers of historical earthquakes in Oklahoma (Hough & Page 2015); Los Angeles, California (Hough & Page 2016); Texas (Frohlich et al. 2016); and Italy (Caciagli et al. 2015). Hough & Page (2015) concluded that locations of M4 and M5 earthquakes in Oklahoma correlated with oil and gas operations in the 1950s. The Caviaga earthquakes in Italy were determined to have occurred in a previously seismically active region, with hypocentral depths in the mid-crust, and are therefore argued to have been naturally triggered (Caciagli et al. 2015). The Gazli, Uzbekistan, earthquakes near a gas-production field may also warrant reconsideration; the primary argument against the earthquakes having been induced is that they migrated through time (Bossu et al. 1996). The sequential triggering sequence evident in the Prague earthquake sequence indicates that an induced earthquake can result in migrating events along faults (e.g., Keranen et al. 2013, Sumy et al. 2014). The Gazli earthquakes appear similar, so the migration cannot be taken as evidence that they were not induced.

Discrimination of Induced Earthquakes: A Summary

Given these many examples, there is, to date, no seismological method that reliably discriminates between tectonic and induced earthquakes. Instead, induced earthquakes typically resemble tectonic earthquakes to a great degree. At the macroscopic scale, the most effective identification of the presence of induced seismicity is still the deviation of regional seismicity rate from the background (e.g., Ellsworth 2013, Llenos & Michael 2013, Atkinson et al. 2016). An understanding of the subsurface structure and permeability distribution, with detailed hydrogeological modeling, is necessary to estimate pressure in the subsurface around wells for further evaluation of induced seismicity. While the lack of distinct characteristics of induced earthquakes may present a great challenge from a practical perspective, it also indicates that induced earthquakes are suitable targets of study to understand natural earthquake triggering, which presents great hazard globally.

METHODS FOR EARLY DETECTION OF FLUID PRESSURE: INSAR AND SUBSURFACE MONITORING

Regions of anthropogenic fluid injection or withdrawal can exhibit surface deformation observable with interferometric synthetic aperture radar (InSAR) satellite data (e.g., Fialko & Simons 2000, Vasco et al. 2010, Ali et al. 2016). However, few areas of the midcontinent of the United States with large volumes of fluid injection show observable surface deformation. In Texas, InSAR data may show ~3 mm/year surface uplift near injection wells near Timpson (**Figure 1**), in the area of an Mw4.8 earthquake in May 2012 (Shirzaei et al. 2016). Satellite data show a coseismic deformation pattern for the 2011 Trinidad, Colorado, earthquake (Barnhart et al. 2014) and for the 2016 Mw5.8 Pawnee, Oklahoma, earthquake (Grandin et al. 2017); however, no preseismic surface uplift was detected at Pawnee despite available satellite images and the expected rise in fluid pressure

prior to the mainshock (e.g., Walter et al. 2017). The lack of detectable surface deformation does not preclude a rise in pressure, since pressures are potentially low and surface deformation may be negligible depending upon the geomechanical, poroelastic, and hydrogeological characteristics of the strata. New satellites have been launched in recent years or are scheduled for launch in the near future (e.g., Davis et al. 2012, Simons 2016), and increased resolution of ground deformation may allow further satellite investigations in regions of fluid injection. Subsurface monitoring of fluid levels in deep wells (e.g., Kroll et al. 2017) also permits detection of changes in fluid pressure through time. Increased future availability of subsurface fluid level measurements would have an immediate impact on understanding subsurface pressure fields and temporal and spatial variability.

MITIGATION AND HAZARD

This review does not include mitigation and hazard assessment of induced seismicity. Mitigation is addressed in a variety of reports and articles (e.g., Natl. Res. Counc. 2013, Atkinson et al. 2015, McGarr et al. 2015, Atkinson 2017, Bommer et al. 2017) and hazard assessment by a variety of groups, including the US Geological Survey (e.g., Petersen et al. 2016) and the Canadian Induced Seismicity Collaboration (e.g., Atkinson et al. 2015, Atkinson 2017). Readers are referred to these sources for information on the important societal impacts, hazard, and mitigation challenges posed by induced seismicity.

CONCLUSIONS AND FUTURE WORK

Induced seismicity is often expected to follow a clear pattern, yet pressure perturbations in the subsurface are controlled by local geology, which varies widely. The far-reaching effects of fluid pressure in sedimentary basins of varying depth, lithology, and structure, combined with low triggering thresholds, create variety in the temporal and spatial patterns of induced seismicity. Statistical analyses of induced seismicity break down if the region used is not large enough to incorporate fluid volumes injected at distant wells and when seismicity occurs following time delays. Seismological discrimination of induced seismicity is not yet routinely possible. Studies of precursory phenomena are exciting directions for future research, including microseismic triggering on faults and geodetic monitoring, which could both aid mitigation and provide insight into earthquake nucleation. However, it is not yet clear that such signals routinely exist, though there is evidence in rare cases for precursory signals before fault failure (e.g., Dodge et al. 1996, Savage et al. 2017a). With dense instrumentation available, and frequent earthquakes, it may be an opportune time to test whether signals are routinely detectable prior to the common M3.0–M4.0 earthquakes in Oklahoma.

Hydrogeological models (including poroelasticity) and resulting estimates of pressure perturbations remain the most reliable way to determine the likelihood of fluid triggering of seismicity. These models, however, rely upon parameters including thickness of injection units and permeability/conductivity that are often not in the public domain, and models often remain fairly simplistic as a result (e.g., Keranen et al. 2014). Improved access to hydrogeological parameters for injection units (both lateral and vertical) would be of strong value for understanding induced seismicity and will require collaboration between industry and academics. Pathways between sedimentary units, where disposal often occurs, and basement, where the majority of earthquakes occur, are poorly constrained and are also a target for future studies. It is important to note that hydrogeological parameters are nonstationary, and shallow groundwater studies indicate that permeability is nonstationary with changes over time (e.g., Manga et al. 2016).

Case studies with varying well operations and local geology indicate that there is no singular parameter that controls the induced earthquake process, and hence, there is no silver bullet for mitigation. As shown by Weingarten et al. (2015), statistical analyses of tens of thousands of injection wells indicate that high-rate injection wells, operating at rates greater than 300,000 barrels/month, are significantly more likely to be associated with earthquakes than are lower-rate wells. This statistical result does not imply that all high-rate wells induce earthquakes, nor does it imply that induced seismicity cannot be triggered by low- or moderate-rate wells; it is instead a probabilistic reflection of the physics of the earthquake process (e.g., **Figure 3**). The overall probability of observing induced seismicity increases with increasing injection rate (Dieterich et al. 2015), and high injection rate is a primary factor in the rise of induced seismicity in the past 10 years. Similarly, natural earthquake rates also scale with the stressing rate (Dieterich 1994).

Improved geological data and hydrogeological models will allow further evaluation of the role of geological setting in induced seismicity—e.g., lithology, structural setting, proximity to basement, and stress state—and such studies will help to guide future development of fluid injection. Such studies will also inform research into earthquake nucleation and fault zone processes and will be useful in understanding seismic risk.

SUMMARY POINTS

1. The permeability structure of the subsurface is as important as the pumping history in determining the fluid pressure perturbations in the subsurface and their temporal-spatial distribution.

2. Induced earthquakes can occur near wells or tens of kilometers from wells and have variable correlation with pumping parameters. A visible, varying temporal signal is not necessarily expected.

3. Induced earthquakes have many similarities to natural earthquakes and provide an opportunity to study earthquake processes with dense sampling.

FUTURE ISSUES

1. Obtaining publicly accessible subsurface data on hydrogeological and geomechanical properties will be necessary for improved characterization of induced seismicity. Many of these data will be most efficiently obtained through collaboration with petroleum operators.

2. Available data on stress state are insufficient for determining whether spatially varying stress fields contribute to spatial variability in induced seismicity. Obtaining reliable, distributed data on principal stress magnitudes, in the public domain, would provide a priori estimates of the proximity of faults to failure and could help determine appropriate regions for long-term, high-volume fluid disposal.

3. The ability of induced seismicity to advance an understanding of earthquake triggering mechanisms relies upon appropriate recording of induced seismicity at the scale at which nucleation processes are occurring, requiring subsurface monitoring and dense surface recording of induced seismicity that has recently become possible with new developments in instrumentation.

LITERATURE CITED

Abercrombie RE. 1995. Earthquake source scaling relationships from −1 to 5 M_L using seismograms recorded at 2.5-km depth. *J. Geophys. Res.* 100:24015–36

Ake J, Mahrer K, O'Connell D, Block L. 2005. Deep-injection and closely monitored induced seismicity at Paradox Valley, Colorado. *Bull. Seismol. Soc. Am.* 95:664–83

Ali ST, Akerley J, Baluyut EC, Cardiff M, Davatzes NC, et al. 2016. Time-series analysis of surface deformation at Brady Hot Springs geothermal field (Nevada) using interferometric synthetic aperture radar. *Geothermics* 61:114–20

Alt RC, Zoback MD. 2016. In situ stress and active faulting in Oklahoma. *Bull. Seismol. Soc. Am.* 107:216–28

Atkinson GM. 2015. Ground-motion prediction equation for small-to-moderate events at short hypocentral distances, with application to induced-seismicity hazards. *Bull. Seismol. Soc. Am.* 105:981–92

Atkinson GM. 2017. Strategies to prevent damage to critical infrastructure due to induced seismicity. *FACETS* 2:374–94

Atkinson GM, Eaton DW, Ghofrani H, Walker D, Cheadle B, et al. 2016. Hydraulic fracturing and seismicity in the Western Canada Sedimentary Basin. *Seismol. Res. Lett.* 87:631–47

Atkinson GM, Ghofrani H, Assatourians K. 2015. Impact of induced seismicity on the evaluation of seismic hazard: some preliminary considerations. *Seismol. Res. Lett.* 86:1009–21

Bachu S. 2008. CO_2 storage in geological media: role, means, status and barriers to deployment. *Prog. Energy Combust. Sci.* 34:254–73

Bader J. 2017. Mapping sandstones of the Inyan Kara Formation for saltwater disposal in North Dakota. *Geo News* 44:6–9. **https://www.dmr.nd.gov/ndgs/documents/newsletter/2017Winter/Mapping%20Sandstones%20of%20the%20Inyan%20Kara%20Formation%20for%20Saltwater%20Disposal%20in%20North%20Dakota.pdf**

Bao X, Eaton DW. 2016. Fault activation by hydraulic fracturing in western Canada. *Science*. **https://doi.org/10.1126/science.aag2583**

Bardwell GE. 1966. Some statistical features of the relationship between Rocky Mountain Arsenal waste disposal and frequency of earthquakes. *Mt. Geol.* 3:37–42

Barnhart WD, Benz HM, Hayes GP, Rubinstein JL, Bergman E. 2014. Seismological and geodetic constraints on the 2011 M_w5.3 Trinidad, Colorado earthquake and induced deformation in the Raton Basin. *J. Geophys. Res.* 119:7923–33

Beller M, Oliver B. 2006. One hundred years of high-throughput *Drosophila* research. *Chromosome Res.* 14:349–62

Benson SM, Cole DR. 2008. CO_2 sequestration in deep sedimentary formations. *Elements* 4:325–31

Bickle MJ. 2009. Geological carbon storage. *Nat. Geosci.* 2:815–19

Bommer JJ, Stafford PJ, Edwards B, Dost B, van Dedem E, et al. 2017. Framework for a ground-motion model for induced seismic hazard and risk analysis in the Groningen gas field, the Netherlands. *Earthq. Spectra* 33:481–98

Bossu R, Grasso JR, Plotnikova LM, Nurtaev B, Frechet J, Moisy M. 1996. Complexity of intracontinental seismic faultings: the Gazli, Uzbekistan, sequence. *Bull. Seismol. Soc. Am.* 86:959–71

BCOGC (B.C. Oil Gas Comm.). 2012. *Investigation of observed seismicity in the Horn River Basin*. Tech. Rep., BCOGC, B.C., Can. **www.bcogc.ca/node/8046/download?documentID=1270**

Caciagli M, Camassi R, Danesi S, Pondrelli S, Salimbeni S. 2015. Can we consider the 1951 Caviaga (Northern Italy) earthquakes as noninduced events? *Seismol. Res. Lett.* 86:1335–44

Carder DS. 1945. Seismic investigations in the Boulder Dam area, 1940–1944, and the influence of reservoir loading on local earthquake activity. *Bull. Seismol. Soc. Am.* 35:175–92

Carrell JR. 2014. *Field-scale hydrogeologic modeling of water injection into the Arbuckle zone of the midcontinent.* Master's Thesis, Dep. Geol. Geophys., Univ. Okla., Norman

Clarke H, Eisner L, Styles P, Turner P. 2014. Felt seismicity associated with shale gas hydraulic fracturing: the first documented example in Europe. *Geophys. Res. Lett.* 41:8308–14

Connolly JAD. 1997. Devolatilization-generated fluid pressure and deformation-propagated fluid flow during prograde regional metamorphism. *J. Geophys. Res.* 102:18149–73

Cox RT. 1991. Possible triggering of earthquakes by underground waste disposal in the El Dorado, Arkansas area. *Seismol. Res. Lett.* 62:113–22

Davis C, Fisk JM. 2017. Mitigating risks from fracking-related earthquakes: assessing state regulatory decisions. *Soc. Nat. Resour.* 30:1009–25

Davis J, Fialko Y, Holt W, Miller M, Owen S, Pritchard M, eds. 2012. *A foundation for innovation: grand challenges in geodesy*. Rep. Long-Range Sci. Goals Geodesy Community Worksh., UNAVCO, Boulder, CO

Davis SD, Frohlich C. 1993. Did (or will) fluid injection cause earthquakes? Criteria for a rational assessment. *Seismol. Res. Lett.* 64:207–24

Davis SD, Pennington WD. 1989. Induced seismic deformation in the Cogdell oil field of west Texas. *Bull. Seismol. Soc. Am.* 79:1477–95

Dieterich JH. 1994. A constitutive law for rate of earthquake production and its application to earthquake clustering. *J. Geophys. Res.* 99:2601–18

Dieterich JH, Richards-Dinger KB, Kroll KA. 2015. Modeling injection-induced seismicity with the physics-based earthquake simulator RSQSim. *Seismol. Res. Lett.* 86:1102–9

Dodge DA, Beroza GC, Ellsworth WL. 1996. Detailed observations of California foreshock sequences: implications for the earthquake initiation process. *J. Geophys. Res.* 101:22371–92

Ekström G, Nettles M, Dziewonski M. 2012. The global CMT project 2004–2010: centroid moment tensors for 13,017 earthquakes. *Phys. Earth Planet. Inter.* 200–1:1–9

Ellsworth WL. 2013. Injection-induced earthquakes. *Science* 341:1225942

Ellsworth WL, Beroza GC. 1995. Seismic evidence for an earthquake nucleation phase. *Science* 268:851–55

Evans DM. 1966. The Denver area earthquakes and the Rocky Mountain Arsenal disposal well. *Mt. Geol.* 3:23–36

Farahbod AM, Kao H, Walker DM, Cassidy JF. 2015. Investigation of regional seismicity before and after hydraulic fracturing in the Horn River Basin, northeast British Columbia. *Can. J. Earth Sci.* 52:112–22

Fialko Y, Simons M. 2000. Deformation and seismicity in the Coso geothermal area, Inyo County, California: observations and modeling using satellite radar interferometry. *J. Geophys. Res.* 105:21781–93

Foulger GR, Wilson MP, Gluyas JG, Julian BR, Davies RJ. 2017. Global review of human-induced earthquakes. *Earth-Sci. Rev.* 178:438–514

Frohlich C, DeShon H, Stump B, Hayward C, Hornbach M, Walter JI. 2016. A historical review of induced earthquakes in Texas. *Seismol. Res. Lett.* 87:1022–38

Frohlich C, Hayward C, Stump B, Potter E. 2011. The Dallas-Fort Worth earthquake sequence: October 2008 through May 2009. *Bull. Seismol. Soc. Am.* 101:327–40

Frohlich C, Walter JI, Gale JF. 2015. Analysis of transportable array (USArray) data shows earthquakes are scarce near injection wells in the Williston Basin, 2008–2011. *Seismol. Res. Lett.* 86:492–99

Gaite B, Ugalde A, Villaseñor A, Blanch E. 2016. Improving the location of induced earthquakes associated with an underground gas storage in the Gulf of Valencia (Spain). *Phys. Earth Planet. Inter.* 254:46–59

Ge S, Liu M, Lu N, Godt JW, Luo G. 2009. Did the Zipingpu Reservoir trigger the 2008 Wenchuan earthquake? *Geophys. Res. Lett.* 36:L20315

Göbel T. 2015. A comparison of seismicity rates and fluid-injection operations in Oklahoma and California: implications for crustal stresses. *Lead. Edge* 34:640–48

Goebel THW, Hosseini SM, Cappa F, Hauksson E, Ampuero JP, et al. 2016. Wastewater disposal and earthquake swarm activity at the southern end of the Central Valley, California. *Geophys. Res. Lett.* 43:1092–99

Goertz-Allmann BP, Gibbons SJ, Oye V, Bauer R, Will R. 2017. Characterization of induced seismicity patterns derived from internal structure in event clusters. *J. Geophys. Res.* 122:3875–94

Gomberg J, Beeler NM, Blanpied ML, Bodin P. 1998. Earthquake triggering by transient and static deformations. *J. Geophys. Res.* 103:24411–26

Grandin R, Vallée M, Lacassin R. 2017. Rupture process of the M_w 5.8 Pawnee, Oklahoma, earthquake from Sentinel-1 InSAR and seismological data. *Seismol. Res. Lett.* 88:994–1004

Grigoli F, Cesca S, Priolo E, Rinaldi AP, Clinton JF, et al. 2017. Current challenges in monitoring, discrimination, and management of induced seismicity related to underground industrial activities: a European perspective. *Rev. Geophys.* 55:310–40

Guglielmi Y, Cappa F, Avouac JP, Henry P, Elsworth D. 2015. Seismicity triggered by fluid injection-induced aseismic slip. *Science* 348:1224–26

Gupta HK. 1985. The present status of reservoir induced seismicity investigations with special emphasis on Koyna earthquakes. *Tectonophysics* 118:257–79

Hacker BR. 1997. Diagenesis and fault valve seismicity of crustal faults. *J. Geophys. Res.* 102:24459–67

Hamilton DH, Meehan RL. 1971. Ground rupture in the Baldwin Hills. *Science* 172:333–44

Harbaugh AW, Langevin CD, Hughes JD, Niswonger RN, Konikow LF. 2017. *MODFLOW-2005 Version 1.12.00: The U.S. Geological Survey Modular Groundwater Model*. US Geol. Surv. Softw. Release, Feb. 3. **https://doi.org/10.5066/F7RF5S7G**

Healy JH, Rubey WW, Griggs DT, Raleigh CB. 1968. The Denver earthquakes. *Science* 161:1301–10

Heidbach O, Tingay M, Barth A, Reinecker J, Kurfeß D, Müller B. 2010. Global crustal stress pattern based on the World Stress Map database release 2008. *Tectonophysics* 482:3–15

Herrmann RB, Park SK, Wang CY. 1981. The Denver earthquakes of 1967–1968. *Bull. Seismol. Soc. Am.* 71:731–45

Hickman SH, Healy JH, Zoback MD. 1985. In situ stress, natural fracture distribution, and borehole elongation in the Auburn geothermal well, Auburn, New York. *J. Geophys. Res.* 90:5497–512

Holland AA. 2013a. Earthquakes triggered by hydraulic fracturing in south-central Oklahoma. *Bull. Seismol. Soc. Am.* 103:1784–92

Holland AA. 2013b. Optimal fault orientations within Oklahoma. *Seismol. Res. Lett.* 84:876–90

Hornbach MJ, Jones M, Scales M, DeShon HR, Magnani MB, et al. 2016. Ellenburger wastewater injection and seismicity in North Texas. *Phys. Earth Planet. Inter.* 261:54–68

Horton S. 2012. Disposal of hydrofracking waste fluid by injection into subsurface aquifers triggers earthquake swarm in central Arkansas with potential for damaging earthquake. *Seismol. Res. Lett.* 83:250–60

Hough SE. 2014. Shaking from injection-induced earthquakes in the central and eastern United States. *Bull. Seismol. Soc. Am.* 104:2619–26

Hough SE, Page M. 2015. A century of induced earthquakes in Oklahoma? *Bull. Seismol. Soc. Am.* 105:2863–70

Hough SE, Page M. 2016. Potentially induced earthquakes during the early twentieth century in the Los Angeles basin. *Bull. Seismol. Soc. Am.* 106:2419–35

Hsieh PA, Bredehoeft JD. 1981. A reservoir analysis of the Denver earthquakes: a case of induced seismicity. *J. Geophys. Res.* 86:903–20

Huang Y, Beroza GC, Ellsworth WL. 2016. Stress drop estimates of potentially induced earthquakes in the Guy-Greenbrier sequence. *J. Geophys. Res.* 121:6597–607

Hubbert MK, Rubey WW. 1959. Role of fluid pressure in mechanics of overthrust faulting. I. Mechanics of fluid-filled porous solids and its application to overthrust faulting. *Geol. Soc. Am. Bull.* 70:115–66

Jackson RB, Vengosh A, Carey JW, Davies RJ, Darrah TH, et al. 2014. The environmental costs and benefits of fracking. *Annu. Rev. Environ. Resour.* 39:327–62

Juanes R, Jha B, Hager BH, Shaw JH, Plesch A, et al. 2016. Were the May 2012 Emilia-Romagna earthquakes induced? A coupled flow-geomechanics modeling assessment. *Geophys. Res. Lett.* 43:6891–97

Keranen KM, Savage HM, Abers GA, Cochran ES. 2013. Potentially induced earthquakes in Oklahoma, USA: links between wastewater injection and the 2011 M_w 5.7 earthquake sequence. *Geology* 41:699–702

Keranen KM, Weingarten M, Abers GA, Bekins BA, Ge S. 2014. Sharp increase in central Oklahoma seismicity since 2008 induced by massive wastewater injection. *Science* 345:448–51

Kim WY. 2013. Induced seismicity associated with fluid injection into a deep well in Youngstown, Ohio. *J. Geophys. Res.* 118:3506–18

King VM, Block LV, Yeck WL, Wood CK, Derouin SA. 2014. Geological structure of the Paradox Valley Region, Colorado, and relationship to seismicity induced by deep well injection. *J. Geophys. Res.* 119:4955–78

Kovach RL. 1974. Source mechanisms for Wilmington oil field, California, subsidence earthquakes. *Bull. Seismol. Soc. Am.* 64:699–711

Kroll KA, Cochran ES, Murray KE. 2017. Poroelastic properties of the Arbuckle Group in Oklahoma derived from well fluid level response to the 3 September 2016 M_w 5.8 Pawnee and 7 November 2016 M_w 5.0 Cushing earthquakes. *Seismol. Res. Lett.* 88:963–70

Lambert C. 2017. *Structural controls on fluid migration and seismic variability in northern Oklahoma*. Master's Thesis, Dep. Earth Atmos. Sci., Cornell Univ., Ithaca, NY

Liu E, Crampin S, Queen JH. 1991. Fracture detection using crosshole surveys and reverse vertical seismic profiles at the Conoco Borehole Test Facility, Oklahoma. *Geophys. J. Int.* 107:449–63

Liu Y, Rice JR. 2007. Spontaneous and triggered aseismic deformation transients in a subduction fault model. *J. Geophys. Res.* 112:B09404

Llenos AL, Michael AJ. 2013. Modeling earthquake rate changes in Oklahoma and Arkansas: possible signatures of induced seismicity. *Bull. Seismol. Soc. Am.* 103:2850–61

Majer EL, Baria R, Stark M, Oates S, Bommer J, et al. 2007. Induced seismicity associated with enhanced geothermal systems. *Geothermics* 36:185–222

Manga M, Wang CY, Shirzaei M. 2016. Increased stream discharge after the 3 September 2016 M_w 5.8 Pawnee, Oklahoma earthquake. *Geophys. Res. Lett.* 43:11588–94

Marsh S, Holland A. 2016. *Comprehensive fault database and interpretive fault map of Oklahoma*. Open-File Rep. OF2, Okla. Geol. Surv., Norman

McGarr A. 2014. Maximum magnitude earthquakes induced by fluid injection. *J. Geophys. Res.* 119:1008–19

McGarr A, Bekins B, Burkardt N, Dewey J, Earle P, et al. 2015. Coping with earthquakes induced by fluid injection. *Science* 347:830–31

Mead TC, Carder DS. 1941. Seismic investigations in the Boulder Dam area in 1940. *Bull. Seismol. Soc. Am.* 31:321–24

Mulargia F, Bizzarri A. 2014. Anthropogenic triggering of large earthquakes. *Sci. Rep.* 4:6100

Murphy EC, Nordeng SH, Juenker BJ, Hoganson JW. 2009. *North Dakota stratigraphic column*. Misc. Ser. 91, N.D. Geol. Surv., Bismarck

Natl. Res. Counc. 2013. *Induced Seismicity Potential in Energy Technologies*. Washington, DC: Natl. Acad. Press

Nicholson C, Wesson RL. 1992. Triggered earthquakes and deep well activities. *Pure Appl. Geophys.* 139:561–78

Norris JQ, Turcotte DL, Moores EM, Brodsky EE, Rundle JB. 2016. Fracking in tight shales: what is it, what does it accomplish, and what are its consequences? *Annu. Rev. Earth Planet. Sci.* 44:321–51

Olson EL, Allen RM. 2005. The deterministic nature of earthquake rupture. *Nature* 438:212

Perilla Castillo P. 2017. *Rock properties derived from analysis of Earth tide strain observed in continuous pressure monitoring of the Arbuckle Group of Oklahoma*. Master's Thesis, Dep. Geol. Geophys., Univ. Okla., Norman

Petersen MD, Mueller CS, Moschetti MP, Hoover SM, Llenos AL, et al. 2016. Seismic-hazard forecast for 2016 including induced and natural earthquakes in the central and eastern United States. *Seismol. Res. Lett.* 87:1327–41

Pratt W, Johnson D. 1926. Local subsidence of the Goose Creek oil field. *J. Geol.* 34:577–90

Rahn PH. 2014. Permeability of the Inyan Kara Group in the Black Hills area and its relevance to a proposed in-situ leach uranium mine. *Proc. S.D. Acad. Sci.* 93:15–32

Raleigh CB, Healy JH, Bredehoeft JD. 1976. An experiment in earthquake control at Rangely, Colorado. *Science* 191:1230–37

Rubinstein JL, Ellsworth WL, McGarr A, Benz HM. 2014. The 2001–present induced earthquake sequence in the Raton basin of northern New Mexico and southern Colorado. *Bull. Seismol. Soc. Am.* 104:2162–81

Rudnicki JW. 1986. Fluid mass sources and point forces in linear elastic diffusive solids. *Mech. Mater.* 5:383–93

Rydelek P, Horiuchi S. 2006. Is earthquake rupture deterministic? *Nature* 442:E5–6

Saffer DM, Tobin HJ. 2011. Hydrogeology and mechanics of subduction zone forearcs: fluid flow and pore pressure. *Annu. Rev. Earth Planet. Sci.* 39:157–86

Savage HM, Keranen KM, Schaff D, Dieck C. 2017a. Possible precursory signals in damage zone foreshocks. *Geophys. Res. Lett.* 44:5411–17

Savage HM, Kirkpatrick JD, Mori JJ, Brodsky EE, Ellsworth WL, et al. 2017b. Scientific Exploration of Induced SeisMicity and Stress (SEISMS). *Sci. Drill.* 23:57–63

Schoenball M, Ellsworth WL. 2017. Waveform-relocated earthquake catalog for Oklahoma and southern Kansas illuminates the regional fault network. *Seismol. Res. Lett.* 88:1252–58

Schultz R, Corlett H, Haug K, Kocon K, MacCormack K, et al. 2016. Linking fossil reefs with earthquakes: geologic insight to where induced seismicity occurs in Alberta. *Geophys. Res. Lett.* 43:2534–42

Scuderi MM, Collettini C. 2016. The role of fluid pressure in induced vs. triggered seismicity: insights from rock deformation experiments on carbonates. *Sci. Rep.* 6:24852

Seeber L, Armbruster J. 1993. Natural and induced seismicity in the Lake Erie-Lake Ontario region: reactivation of ancient faults with little neotectonic displacement. *Géog. Phys. Quat.* 47:363–78

Seeber L, Armbruster JG, Kim WY. 2004. A fluid-injection-triggered earthquake sequence in Ashtabula, Ohio: implications for seismogenesis in stable continental regions. *Bull. Seismol. Soc. Am.* 94:76–87

Segall P. 1985. Stress and subsidence resulting from subsurface fluid withdrawal in the epicentral region of the 1983 Coalinga earthquake. *J. Geophys. Res.* 90:6801–16

Segall P. 1989. Earthquakes triggered by fluid extraction. *Geology* 17:942–46

Segall P, Lu S. 2015. Injection-induced seismicity: poroelastic and earthquake nucleation effects. *J. Geophys. Res.* 120:5082–103

Shelly DR, Moran SC, Thelen WA. 2013. Evidence for fluid-triggered slip in the 2009 Mount Rainier, Washington earthquake swarm. *Geophys. Res. Lett.* 40:1506–12

Shirzaei M, Ellsworth WL, Tiampo KF, González PJ, Manga M. 2016. Surface uplift and time-dependent seismic hazard due to fluid injection in eastern Texas. *Science* 353:1416–19

Sibson RH. 1992. Implications of fault-valve behaviour for rupture nucleation and recurrence. *Tectonophysics* 211:283–93

Sibson RH. 2000. Fluid involvement in normal faulting. *J. Geodyn.* 29:469–99

Simons M. 2016. *InSAR geodesy: the next phase*. Presented at Am. Geophys. U. Fall Meet., Dec. 12–16, San Francisco, CA. Abstr. G34A-01

Simpson DW, Leith W. 1985. The 1976 and 1984 Gazli, USSR, earthquakes—were they induced? *Bull. Seismol. Soc. Am.* 75:1465–68

Skoumal RJ, Brudzinski MR, Currie BS. 2015a. Distinguishing induced seismicity from natural seismicity in Ohio: demonstrating the utility of waveform template matching. *J. Geophys. Res.* 120:6284–96

Skoumal RJ, Brudzinski MR, Currie BS. 2015b. Earthquakes induced by hydraulic fracturing in Poland Township, Ohio. *Bull. Seismol. Soc. Am.* 105:189–97

Skoumal RJ, Brudzinski MR, Currie BS. 2016. An efficient repeating signal detector to investigate earthquake swarms. *J. Geophys. Res.* 121:5880–97

Smalley PC, Muggeridge AH. 2010. Reservoir compartmentalization: Get it before it gets you. *Geol. Soc. Lond. Spec. Publ.* 347:25–41

Stabile TA, Giocoli A, Perrone A, Piscitelli S, Lapenna V. 2014. Fluid injection induced seismicity reveals a NE dipping fault in the southeastern sector of the High Agri Valley (southern Italy). *Geophys. Res. Lett.* 41:5847–54

Stein RS. 1999. The role of stress transfer in earthquake occurrence. *Nature* 402:605–9

Stewart FL, Ingelson A. 2017. Regulating energy innovation: US responses to hydraulic fracturing, wastewater injection and induced seismicity. *J. Energy Nat. Resour. Law* 35:109–46

Suckale J. 2009. Induced seismicity in hydrocarbon fields. *Adv. Geophys.* 51:55–106

Suckale J. 2010. Moderate-to-large seismicity induced by hydrocarbon production. *Lead. Edge* 29:310–19

Sumy DF, Cochran ES, Keranen KM, Wei M, Abers GA. 2014. Observations of static Coulomb stress triggering of the November 2011 M5.7 Oklahoma earthquake sequence. *J. Geophys. Res.* 119:1904–23

Sumy DF, Neighbors CJ, Cochran ES, Keranen KM. 2017. Low stress drops observed for aftershocks of the 2011 M_w 5.7 Prague, Oklahoma, earthquake. *J. Geophys. Res.* 122:3813–34

Tester JW, Anderson BJ, Batchelor AS, Blackwell DD, DiPippo R, et al. 2006. *The future of geothermal energy: impact of enhanced geothermal systems (EGS) on the United States in the 21st century*. Rep. INL/EXT-06–11746, Mass. Inst. Technol. and Dep. Energy, Ida. Natl. Lab., Idaho Falls

Townend J, Zoback MD. 2000. How faulting keeps the crust strong. *Geology* 28:399–402

Valoroso L, Improta L, Chiaraluce L, Di Stefano R, Ferranti L, et al. 2009. Active faults and induced seismicity in the Val d'Agri area (Southern Apennines, Italy). *Geophys. J. Int.* 178:488–502

van der Elst NJ, Page MT, Weiser DA, Goebel TH, Hosseini SM. 2016. Induced earthquake magnitudes are as large as (statistically) expected. *J. Geophys. Res.* 121:4575–90

van der Elst NJ, Savage HM, Keranen KM, Abers GA. 2013. Enhanced remote earthquake triggering at fluid-injection sites in the midwestern United States. *Science* 341:164–67

van Thienen-Visser K, Breunese JN. 2015. Induced seismicity of the Groningen gas field: history and recent developments. *Lead. Edge* 34:664–71

Vasco DW, Rucci A, Ferretti A, Novali F, Bissell RC, et al. 2010. Satellite-based measurements of surface deformation reveal fluid flow associated with the geological storage of carbon dioxide. *Geophys. Res. Lett.* 37:L03303

Viesca RC, Garagash DI. 2015. Ubiquitous weakening of faults due to thermal pressurization. *Nat. Geosci.* 8:875

Walsh FR, Zoback MD. 2015. Oklahoma's recent earthquakes and saltwater disposal. *Sci. Adv.* 1:e1500195

Walter JI, Chang JC, Dotray PJ. 2017. Foreshock seismicity suggests gradual differential stress increase in the months prior to the 3 September 2016 M_w 5.8 Pawnee earthquake. *Seismol. Res. Lett.* 88:1032–39

Weatherley DK, Henley RW. 2013. Flash vaporization during earthquakes evidenced by gold deposits. *Nat. Geosci.* 6:294

Weingarten M, Ge S, Godt JW, Bekins BA, Rubinstein JL. 2015. High-rate injection is associated with the increase in US mid-continent seismicity. *Science* 348:1336–40

Wells DL, Coppersmith KJ. 1994. New empirical relationships among magnitude, rupture length, rupture width, rupture area, and surface displacement. *Bull. Seismol. Soc. Am.* 84:974–1002

Wibberley CA, Gonzalez-Dunia J, Billon O. 2017. Faults as barriers or channels to production-related flow: insights from case studies. *Pet. Geosci.* 23:134–47

Wilson MP, Davies RJ, Foulger GR, Julian BR, Styles P, et al. 2015. Anthropogenic earthquakes in the UK: a national baseline prior to shale exploitation. *Mar. Pet. Geol.* 68:1–17

Yeck WL, Weingarten M, Benz HM, McNamara DE, Bergman EA, et al. 2016. Far-field pressurization likely caused one of the largest injection induced earthquakes by reactivating a large preexisting basement fault structure. *Geophys. Res. Lett.* 43:10198–207

Yenier E, Atkinson GM, Sumy DF. 2017. Ground motions for induced earthquakes in Oklahoma. *Bull. Seismol. Soc. Am.* 107:198–215

Yielding G, Needham T, Jones H. 1996. Sampling of fault populations using sub-surface data: a review. *J. Struct. Geol.* 18:135–46

Zakharova NV, Goldberg DS. 2014. In situ stress analysis in the northern Newark Basin: implications for induced seismicity from CO_2 injection. *J. Geophys. Res.* 119:2362–74

Zhang Y, Person M, Rupp J, Ellett K, Celia MA, et al. 2013. Hydrogeologic controls on induced seismicity in crystalline basement rocks due to fluid injection into basal reservoirs. *Groundwater* 51:525–38